(Preprint) AAS 13-339

PRELIMINARY DESIGN CONSIDERATIONS FOR ACCESS AND OPERATIONS IN EARTH-MOON L_1/L_2 ORBITS

David C. Folta*, Thomas A. Pavlak†, Amanda F. Haapala†
and Kathleen C. Howell‡

Within the context of manned spaceflight activities, Earth-Moon libration point orbits could support lunar surface operations and serve as staging areas for future missions to near-Earth asteroids and Mars. This investigation examines preliminary design considerations including Earth-Moon L_1/L_2 libration point orbit selection, transfers, and stationkeeping costs associated with maintaining a spacecraft in the vicinity of L_1 or L_2 for a specified duration. Existing tools in multi-body trajectory design, dynamical systems theory, and orbit maintenance are leveraged in this analysis to explore end-to-end concepts for manned missions to Earth-Moon libration points.

INTRODUCTION

In 2010, the two ARTEMIS spacecraft became the first man-made vehicles to exploit trajectories in the vicinity of an Earth-Moon (EM) libration point, operating successfully in this dynamical regime from August 2010 through July 2011.[1,2] The EM libration points offer locations for platforms for scientific observation and/or communication relays, implying that these locations will likely garner increased attention in the coming years. In 2011, libration point missions were included as part of "The Global Exploration Roadmap"[3] released by NASA and, as recently as June 2012, NASA has identified the collinear L_1 and L_2 libration points in the EM system as potential locations of interest for future human space operations.[4] Within the context of manned spaceflight activities, orbits near the EM L_1 and/or L_2 points could support lunar surface operations and serve as staging areas for future missions to near-Earth asteroids and Mars.

The dynamical environment within the EM system is complex and, as a consequence, trajectory design and operations in the vicinity of the EM L_1 and L_2 points are nontrivial. In this investigation, some issues that are significant for preliminary design are explored, including EM L_1/L_2 libration point orbit selection, transfers to and from these locations, as well as stationkeeping (SK) costs associated with maintaining a spacecraft in the vicinity of L_1 and/or L_2 over a specified duration. Existing tools in the areas of multi-body trajectory design, dynamical systems theory, and orbit maintenance are leveraged in this analysis to explore end-to-end concepts for manned missions to EM libration points.

A wealth of design possibilities exist for transfers from Earth to the L_1/L_2 region. However, in the EM multi-body environment, and in constrast to robotic missions, the transfer time of flight

*Aerospace Engineer, NASA Goddard Space Flight Center, Greenbelt, Maryland 20771.
†Graduate Student, Purdue University, School of Aeronautics and Astronautics, West Lafayette, Indiana 47907.
‡Hsu Lo Professor of Aeronautical and Astronautical Engineering, Purdue University, School of Aeronautics and Astronautics, West Lafayette, Indiana 47907. Fellow AAS; Fellow AIAA.

(TOF) for human missions to the vicinity of the EM libration points is strictly constrained by the life support systems aboard the spacecraft. The Orion spacecraft, for example, has an operational maximum round-trip duration of 21 days.[5] Thus, the trajectory solutions must be both low-cost, in terms of required propellant, and of reasonable duration. Preliminary transfer design is conducted within the context of the circular restricted three-body (CR3B) problem to utilize elements of dynamical systems theory including Poincaré mapping and invariant manifolds when applicable. Other known solutions in the CR3B problem, such as three-body free return trajectories, are also exploited. Flexible multiple shooting algorithms are employed to blend multiple segments into continuous trajectories while constraining the location and/or magnitude of any ΔV maneuvers. Both direct transfers to the regions near the EM L_1 and L_2 points as well as transfer options incorporating a close lunar passage are investigated in terms of the CR3B as well as higher-fidelity ephemeris models that include the effects of lunar eccentricity and solar gravity.

BACKGROUND

Circular Restricted Three-Body Model

For preliminary analysis, the CR3B model[6] is assumed as the force model. The focus of this investigation is on solutions in the Earth-Moon (EM) system. Then, the motion of a spacecraft, assumed massless, is determined by the gravitational forces of the Earth and the Moon, each represented as a point mass. The orbits of the Earth and Moon are assumed to be circular relative to the system barycenter. A barycentric rotating frame is defined such that the rotating x-axis is directed from the Earth to the Moon, the z-axis is parallel to the direction of the angular velocity of the primary system, and the y-axis completes the right-handed, orthonormal triad. The position of the spacecraft relative to the EM barycenter is defined in terms of rotating coordinates as $\boldsymbol{r} = [x, y, z]$, where bold symbols denote vector quantities. The mass parameter is defined as $\mu = \frac{m_1}{m_1+m_2}$, where m_1 and m_2 correspond to the mass of the Earth and Moon, respectively. The first-order, nondimensional, vector equation of motion is

$$\dot{\boldsymbol{x}} = \boldsymbol{f}(\boldsymbol{x}), \tag{1}$$

where the vector field, $\boldsymbol{f}(\boldsymbol{x})$, is defined

$$\boldsymbol{f}(\boldsymbol{x}) = \left[\dot{x}, \dot{y}, \dot{z}, 2n\dot{y} + U_x, -2n\dot{x} + U_y, U_z\right], \tag{2}$$

noting that the nondimensional mean motion of the primary system is $n = 1$. In Equation (2), $U(x, y, z, n) = \frac{1-\mu}{d} + \frac{\mu}{r} + \frac{1}{2}n^2\left(x^2 + y^2\right)$ is the pseudo-potential function, with the non-dimensional Earth-spacecraft and Moon-spacecraft distances written as d and r, respectively, and the quantities U_x, U_y, U_z represent partial derivatives of U with respect to rotating position coordinates. In this analysis, Dormand-Prince 8(9) and Adams-Bashforth-Moulton numerical integration schemes are utilized to propagate the first-order equations of motion. The only known integral of the motion is the Jacobi constant, evaluated as $C = 2U - v^2$, where $v = \left(\dot{x}^2 + \dot{y}^2 + \dot{z}^2\right)^{1/2}$; this quantity is a constant of the motion in the rotating frame.

Libration Point Orbits and Their Associated Invariant Manifolds

The CR3B model admits five equilibrium points, including three collinear libration points, L_1, L_2, and L_3, that lie along the x-axis, and two equilateral points, L_4 and L_5. Several types of periodic and quasi-periodic orbits exist in the vicinity of the collinear points, including the periodic

Lyapunov, vertical, and halo families of orbits, as well as the quasi-periodic Lissajous and quasi-halo orbits. Many techniques exist to compute these orbits.[7–11] For unstable orbits, there exist stable and unstable manifolds that represent flow toward and away from the orbit. To compute the global manifolds associated with unstable periodic orbits, an initial step off the orbit onto a manifold is generated and numerically propagated in the full nonlinear equations of motion (see Grebow (2006)[11] for details). An example of EM L_1 manifolds associated with a planar Lyapunov orbit at a specified value of C appears in Figure 1.

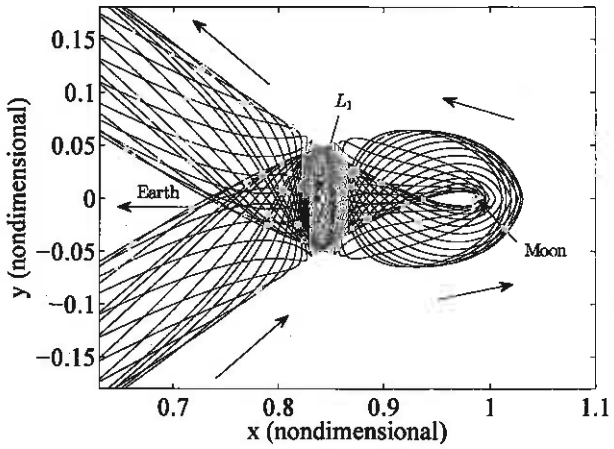

Figure 1. Invariant manifold associated with an EM L_1 Lyapunov orbit

Poincaré Maps

To provide a more complete picture of the libration point orbits that exist for a particular energy level (value of C), it is useful to employ Poincaré maps. The use of a Poincaré map allows an n-dimensional continuous-time system to be reduced to a discrete-time system of $(n-1)$-dimensions. By additionally constraining the Jacobi constant, C , the problem is reduced to $(n-2)$-dimensions and the map is represented in 4-D. To generate a Poincaré map, a surface-of-section, Σ, is defined such that Σ is transversal to the flow. Initial conditions are then integrated using Equations (1) and (2), and crossings of Σ are recorded and displayed. As an example, the map in Figure 2 is produced to resemble maps demonstrated by Gómez et al. (2001),[12] as well as Kolemen et al. (2007).[10] Periodic and quasi-periodic orbits are computed, and crossings of the surface $\Sigma = \{\boldsymbol{x} : z = 0\}$ are recorded to generate the map. The image in Figure 2 represents a projection of the map onto the $x - y$ plane. This map corresponds to a value of $C = 3.080$, and displays crossings of the planar Lyapunov orbit (green), vertical orbit (dark blue), and the northern and southern halo orbits (magenta), all at the given value of C. In this projection, the northern and southern halo orbits share the same crossings of the map. Surrounding the periodic vertical orbit are the quasi-periodic Lissajous orbits. The quasi-halo orbits lie in the center subspace of the central halo orbit. Examples of small and large northern quasi-halo orbits appear in red and orange, respectively; a large Lissajous orbit is represented in cyan. Similar maps exist for varying values of C, and may also be computed in the vicinity of L_2.

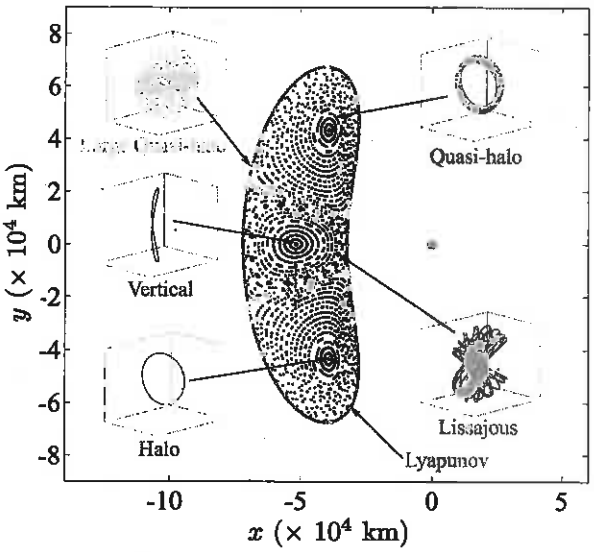

Figure 2. Poincaré map depicting periodic and quasi-periodic libration point orbit structures in the vicinity of L_1 in the EM system for $C = 3.080$

Ephemeris Model

While the circular restricted three-body model incorporates the dominant multi-body gravitational forces, many collinear libration point orbits are dynamically unstable and even small perturbations can significantly alter their evolution. Thus, it is important to analyze Earth to L_1/L_2 transfers in higher-fidelity ephemeris models as well. In this analysis, selected transfer trajectories in the CR3B model are transitioned to an Earth-Moon-Sun point mass ephemeris model incorporating lunar eccentricity and solar gravity. In practice, the traditional N-body relative equations of motion are written in first-order form as in Equation (1) and numerically integrated. Relative position and velocity information for the gravitational bodies is obtained from the DE405 planetary ephemerides. Employing higher-fidelity ephemeris modeling, the transfers from Earth to the regions near the L_1 and L_2 libration points can be examined to explore the effects of lunar eccentricity, solar gravity, and equatorial launch inclination on ΔV cost, time of flight, and orbit evolution.

Stationkeeping Strategy

Many orbits in the vicinity of EM L_1 and L_2 libration points are unstable and must be maintained with stationkeeping maneuvers executed at regular intervals. Thus, stationkeeping strategies are an integral component of human operations near the EM libration points and should be considered during preliminary mission design activities along with the transfer. In this analysis, the long-term stationkeeping strategy previously detailed by Pavlak and Howell[13] is employed to compute stationkeeping costs for L_1 and L_2 libration point orbits of various types and sizes. Fundamentally, the long-term stationkeeping strategy utilizes a multi-revolution reference solution and a multiple shooting algorithm to design stationkeeping ΔV maneuver many revolutions into the future. Optimal maneuvers are designed using sequential quadratic programming (SQP). In an effort to simulate real-world operational stationkeeping conditions, randomly-distributed simulated modeling/navigation and maneuver execution errors are added to each designed stationkeeping ΔV maneuver. Each stationkeeping analysis is repeated hundreds of times in Monte Carlo simulation

approximate average operational stationkeeping ΔV costs.

TRANSFER TRAJECTORY DESIGN

The selection of a libration point orbit is influenced by many factors. Besides any given mission requirements, the propellant and TOF costs associated with transfers to these orbits are critical. These costs can vary significantly between L_1 and L_2 orbits, as well as for different values of C and different orbit types.

A variety of approaches exist to locate transfers to libration point orbits near L_1 and L_2.[14] Two solution types are explored in this investigation: (1) direct two-burn transfers that insert onto the orbit at the negative ($\dot{y} < 0$) x-axis crossing; and (2) three-burn transfers with a lunar passage and an "intermediate multi-body arc" that links an outbound Earth segment to a libration point orbit.

Two-Burn Transfers

Direct, two-burn transfers offer transfer times to libration point orbits from LEO on the order of 4-7 days. These transfers include one maneuver (ΔV_1) to depart from LEO, and a second maneuver (ΔV_2) to enter the libration point orbit. Such transfers have been previously investigated by Rausch (2005)[15] for both L_1 and L_2 halo orbits. Parker and Born (2007)[16] extensively examine the costs associated with transfer to halo orbits in the vicinity of L_1 and L_2. To compute direct transfers from circular LEO in this study, a conic initial guess is located that provides direct insertion from the conic at apogee into a libration point orbit at a specified location. This initial guess is refined within the framework of the CR3BP via optimization, while enforcing that the transfer depart from 200 km LEO. To implement the optimization process, fmincon is employed in MATLAB using Sequential Quadratic Programming (SQP) as the solution algorithm, and the cost function is defined as the magnitude of ΔV_2. To aid convergence, the initial guess is discretized into multiple segments and full-state continuity is enforced between subsequent segments; constraining the LEO departure to be tangential additionally improves the convergence of the optimizer.

The costs associated with direct transfers to libration point orbits vary with many parameters, such as orbit type, orbit energy level, the insertion location along an orbit, or whether an L_1 or L_2 orbit is considered. Due to the direction of flow of orbits in the vicinity of the libration points, orbit insertion on the negative ($\dot{y} < 0$) x-axis crossings generally requires less ΔV. For quasi-periodic orbits, an infinite number of such crossings exist; however, the cost associated with direct transfers to each of these crossings varies. Consider direct transfers to the families of quasi-halo and Lissajous orbits that exist for a value of $C = 3.15$. For a particular orbit within this set, the ΔV required for a direct transfer is greatly affected by the insertion location that is selected along the orbit. A 'large' L_1 quasi-halo orbit is depicted in Figure 3(a); the orbit insertion locations considered are plotted in color in the figure. The magnitude of the second maneuver, ΔV_2, and time-of-flight, t_b, for direct transfers to these locations appears in Figure 3(b). The colors in Figure 3 correspond to the magnitude of the quantity $\Delta V_{tot} = \Delta V_1 + \Delta V_2$. Analogous plots are presented for a large L_1 Lissajous orbit in Figures 3(c) and 3(d). In both cases, decreasing the z-amplitude of the x-axis crossing employed as the orbit insertion location provides a reduction in the ΔV_{tot} required for the transfer. While no constraints on the departure inclination are applied for these transfers, enforcing $i = 28.5°$ at LEO departure appears to have only a minor effect on the transfer costs in Figure 3. Selecting a smaller quasi-halo or Lissajous orbit yields a different set of x-axis crossings and, thus, the required ΔV will vary. Consider the entire L_1 family of northern halo/quasi-halo orbits that exists for a value of $C = 3.15$. To determine the relative costs associated with different orbits

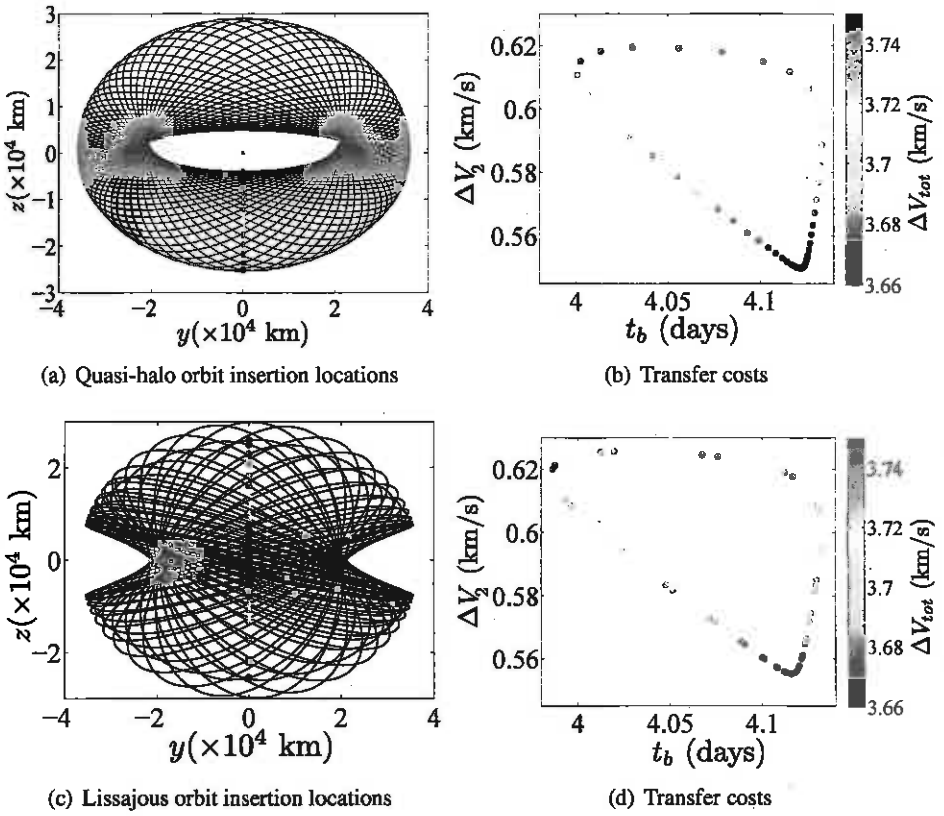

(a) Quasi-halo orbit insertion locations

(b) Transfer costs

(c) Lissajous orbit insertion locations

(d) Transfer costs

Figure 3. Costs associated with direct transfers to large L_1 quasi-halo and Lissajous orbits for $C = 3.15$.

within this family, three orbits are selected for comparison: the periodic halo orbit, a 'medium' sized quasi-halo orbit, and the same 'large' quasi-halo orbit that appears in Figure 3(a). Direct transfers to the these orbits appear in Figure 4; the libration point orbits are plotted in Figures 4(b), 4(d), and 4(f) with the insertion locations indicated by red dots. Increasing the orbit size serves to reduce the lowest z-amplitude that is achieved for the x-axis crossings, thus reducing the required ΔV for direct transfer.

By varying the energy level associated with a particular libration point orbit, the cost of direct transfer can change drastically. To examine this effect, the costs to transfer to Lyapunov, halo, quasi-halo, vertical and Lissajous orbits are computed for a variety of values of the Jacobi constant, C. The transfer time, t_b, and magnitude of the maneuver ΔV_2 corresponding to direct transfers to subsets of the L_1 families of halo, quasi-halo, vertical, and Lissajous orbits are represented by the colored dots in Figure 5(a), where the color of each point indicates the Jacobi constant value associated with the corresponding libration point orbit. Transfers to the planar Lyapunov orbits lie along the dashed black curve. Similarly, transfer costs associated with the L_2 families of halo and quasi-halo orbits appear in Figure 5(b); vertical and Lissajous orbits are not considered due to line-of-sight violations caused by the Moon, although such violations also occur for many of the L_2 quasi-halo orbits. Because nearly planar revolutions are selected for insertion into the quasi-periodic orbits, the curves representing the costs associated with transfers to the quasi-halo and Lissajous orbits converge near the Lyapunov orbit family curve. The costs associated with direct transfer

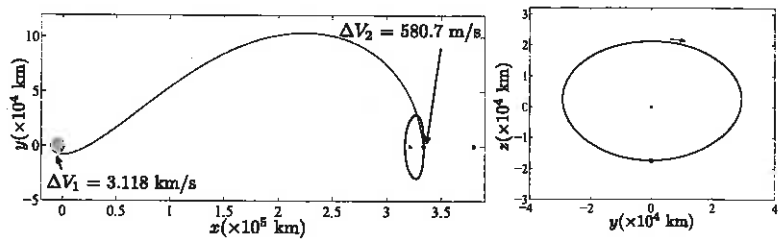

(a) Transfer into a halo orbit, $t_b = 4.09$ days

(b) Halo orbit insertion location

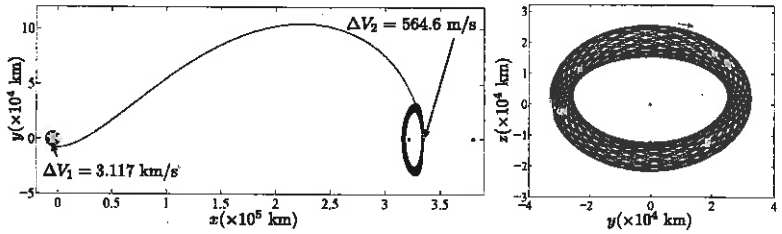

(c) Transfer into a medium quasi-halo orbit, $t_b = 4.11$ days

(d) Medium quasi-halo orbit insertion location

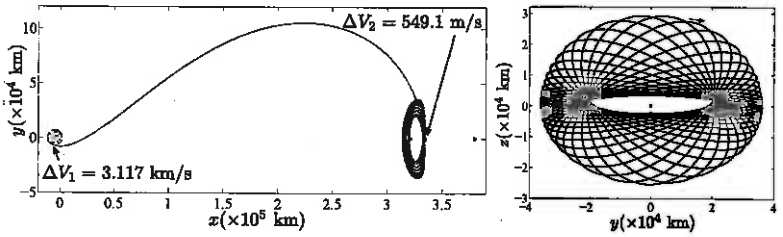

(e) Transfer into a large quasi-halo orbit, $t_b = 4.12$ days

(f) Large quasi-halo orbit insertion location

Figure 4. Direct transfers to L_1 libration point orbits for $C = 3.15$.

to smaller quasi-halo/Lissajous orbits lie on the surface between the halo/vertical and large quasi-halo/Lissajous curves. Sample orbits from the L_1 families are plotted in Figure 6 to demonstrate the relative orbit sizes; red dots indicate the selected orbit insertion locations. It should be noted that the costs associated with direct transfers to the vertical orbits are the same if the southern-most location is selected for orbit insertion.

Three-Burn Transfers with Lunar Passage

In addition to direct transfers, the Earth-to-L_1/L_2 design space can also be augmented with lunar assisted transfers that leverage "close" lunar passage to insert into the desired libration point orbit. This analysis incorporates a segment of a lunar free return trajectory to take the spacecraft from circular LEO to the vicinity of the Moon as part of an initial guess for a differential corrector. Free return trajectories are utilized in this investigation for two reasons: (1) if desired, the free return can be explicitly preserved in the converged solution to ensure that, if the spacecraft malfunctions and the libration point orbit phase of the mission is aborted, no maneuvers are required to return the crew safely to Earth and (2) from a mission design prospective, free return trajectories are

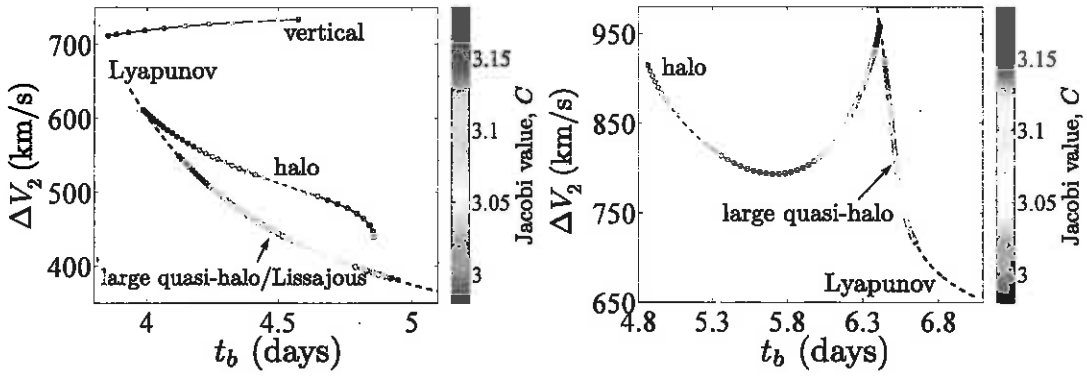

(a) L_1 orbit families (b) L_2 orbit families

Figure 5. Costs associated with transfers to L_1 and L_2 libration point orbits for various values of C.

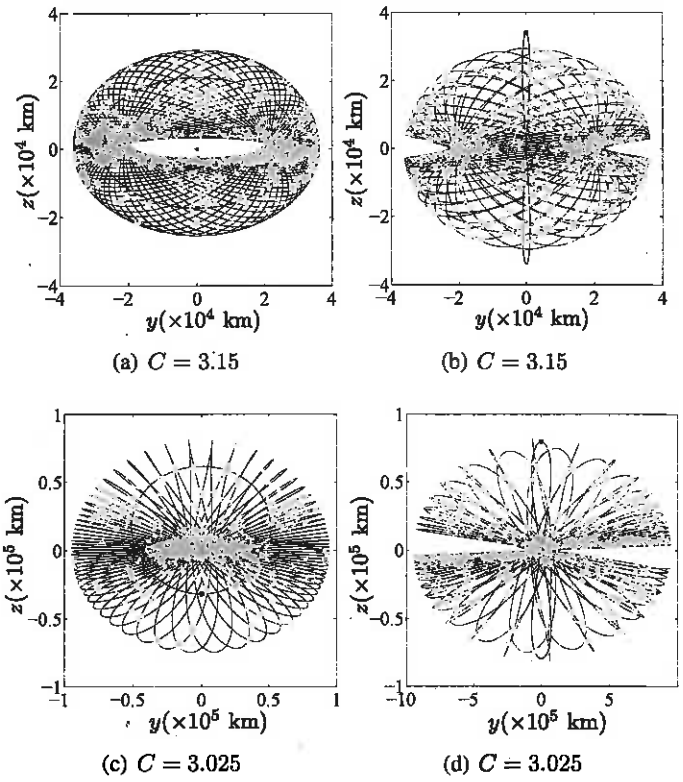

(a) $C = 3.15$ (b) $C = 3.15$

(c) $C = 3.025$ (d) $C = 3.025$

Figure 6. Halo (magenta), quasi-halo (green), vertical (dark blue), and Lissajous (cyan) orbits in the vicinity of L_1 for various values of C.

well-understood and provide an abundance of transfer design options. Families of cislunar and circumlunar free return trajectories are depicted in Figure 7. The cislunar trajectories (in gray) cross the $x - z$ plane between the Earth and the Moon while the circumlunar trajectories (in black) travel around the far side of the Moon before returning to Earth.

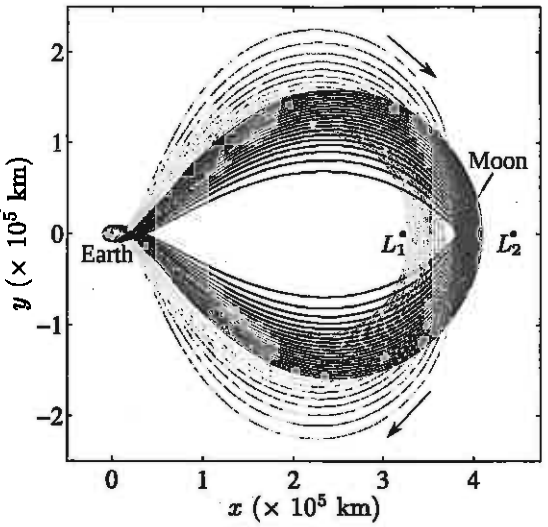

Figure 7. Family of circumlunar free return trajectories

Three-burn transfers with close lunar passage are capable of transitioning a spacecraft from the vicinity of Earth to either EM L_1 or L_2, however, transfers to the former are considered first in this investigation. In Figure 8, it is first interesting to note that, in general, circumlunar free return trajectories and the stable manifolds associated with EM L_1 libration point orbits intersect on the lunar far side but in opposite directions. Thus, insertion from the free return trajectory onto the stable

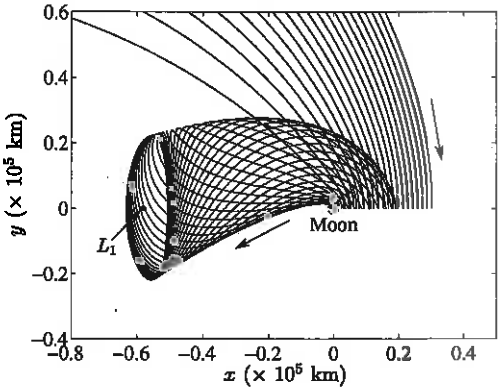

Figure 8. Stable L_1 Lyapunov manifolds

manifold would require prohibitively large ΔV maneuvers to completely reverse the spacecraft's direction of travel. Instead, a multi-body "intermediate arc" can be incorporated within the context of a three-burn transfer scheme to link the free return transfer segment with the desired libration point orbit. A sample initial guess strategy for a transfer from circular LEO to an EM southern L_1 halo orbit appears in Figure 9. Employing this initial guess strategy, three burn Earth-L_1 transfer trajectories are constructed for a range of trajectories in the EM L_1 southern halo family with z-amplitudes that vary from 5000 km (Orbit 1) to 77,000 km (Orbit 10). Since the first maneuver, ΔV_1, is dependent on the low Earth parking orbit being used, only the sum of the second two maneuvers, $\Delta V_2 + \Delta V_3$ is reported in this analysis. Note, however, that if it is assumed that the spacecraft

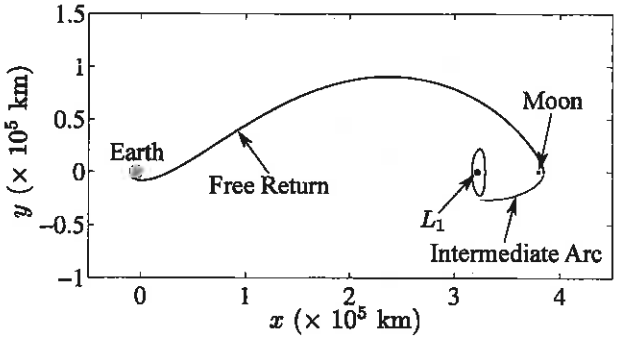

Figure 9. Three-burn EM L_1 transfer initial guess strategy

is departing a 200-km altitude circular Earth parking orbit, ΔV_1 costs are typically slightly over 3.1 km/s. In each case, once an initial transfer is converged, a differential corrections continuation procedure is implemented to reduce the combined $\Delta V_2 + \Delta V_3$ cost. To ensure a fair comparison amongst the CR3B EM-L_1 and EM-L_2 in this study, the perilune altitude of each trajectory is fixed at 200 km. The first converged three-burn EM-L_1 transfer trajectory to a final EM L_1 southern halo orbit that possesses a maximum z-amplitude of approximately 5000 km is depicted in Figure 10. This initial EM-L_1 transfer trajectory has an intermediate ΔV cost of $\Delta V_2 + \Delta V_3 = 516$ m/s

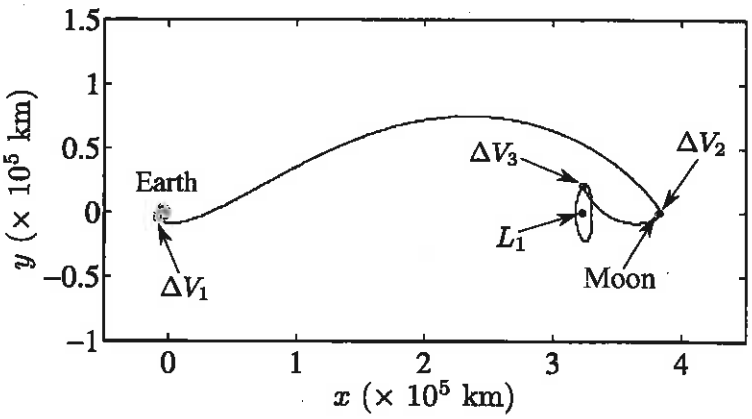

Figure 10. Example three-burn Earth-L_1 transfer

and a time of flight of 4.87 days. Utilizing this converged solution as an initial guess, a differential corrector used to compute a transfer to the second EM L_1 southern halo orbit under consideration. This process is repeated for each halo orbit of interest in the family and the results of all of the transfers are summarized in Table 1. The most notable result is that, as the algorithm steps through the EM L_1 southern halo family, the intermediate ΔV cost decreases at the cost of increased time of flight.

Once a desired Earth-L_1 transfer trajectory is computed, a complete end-to-end Earth-L_1-Earth design is achieved by connecting the EM L_1 libration point orbit with an Earth-bound leg of a cislunar free return trajectory as demonstrated in Figure 11. This round trip trajectory is comprised of a three-burn transfer that inserts into a 5000-km z-amplitude EM L_1 southern halo orbit for approximately one day before a fourth maneuver is executed to place the spacecraft on a Earth-

Table 1. EM-L_1 transfer ΔV costs

Orbit No.	ΔV_2 (m/s)	ΔV_2 (m/s)	$\Delta V_2 + \Delta V_3$ (m/s)	TOF (days)
1	268.87	247.14	516.01	4.87
2	271.80	240.63	512.43	5.09
3	271.58	188.10	459.68	5.42
4	266.90	130.17	397.07	5.80
5	263.66	96.61	360.27	6.40
6	254.10	82.90	337.00	7.50
7	245.13	80.22	325.35	7.67
8	235.08	79.12	314.20	7.81
9	228.41	80.17	308.58	7.61
10	231.46	80.35	311.81	7.27

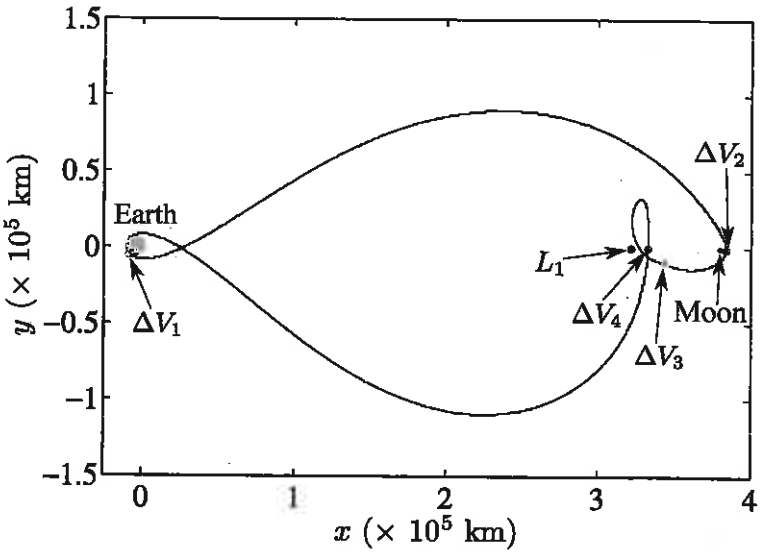

Figure 11. Example Earth-L_1-Earth transfer

bound return path. The total ΔV cost – not including the Earth parking orbit departure maneuver – is approximately 1.07 km/s and the total time of flight is 15.8 days which is well within the stipulated 21-day limit for a human libration point orbit mission design.

This investigation next demonstrates the computation of three-burn Earth-L_2 transfer incorporating close lunar passage using a method very similar to the one discussed previously for Earth-L_1 trajectories. The only difference between the two design strategies is that, to reach L_2, a cislunar free return trajectory is employed as part of the initial guess so that the spacecraft will pass close to the near side of the Moon as it travels towards EM L_2. The modified initial guess scheme is demonstrated in Figure 12 Three-burn Earth-L_2 transfer trajectories are computed for select members of the EM L_2 southern halo family whose z-amplitudes range from 5000 km (Orbit 1) to 76,000 km (Orbit 8). Like the Earth-L_1 transfers, the perilune altitude is constrained to 200 km for purposes of comparison. The three-burn transfer to the initial EM L_2 southern halo orbit of interest appears in Figure 13. Employing a differential corrector and continuation procedure, the intermediate ΔV

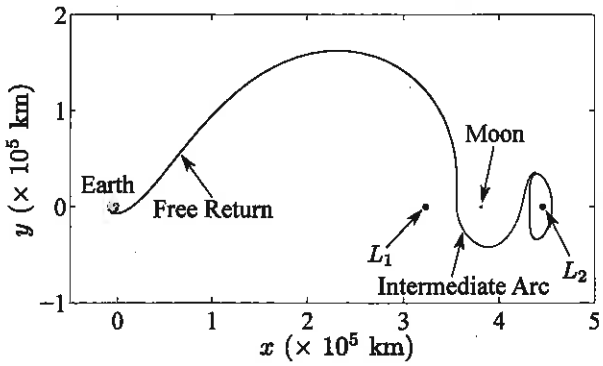

Figure 12. Three-burn EM L_2 transfer initial guess strategy

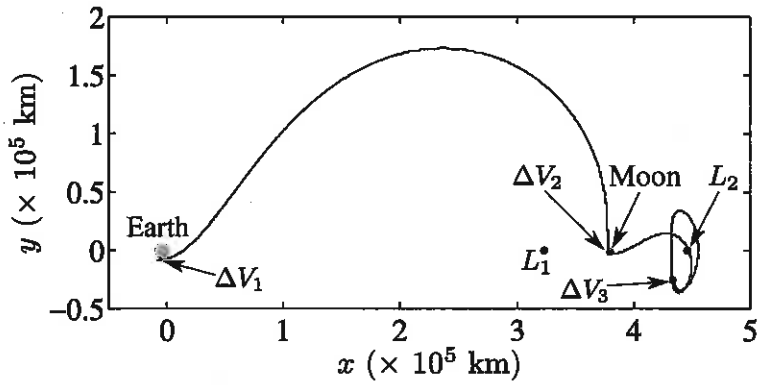

Figure 13. Example three-burn Earth-L_2 transfer

cost is reduced to a value of $\Delta V_2 + \Delta V_3 = 202$ m/s corresponding to a time of flight of 14.70 days. This Earth-L_2 transfer approach sharply contrasts the two-burn direct Earth-L_2 transfers presented in the previous section in that this transfer possesses a significantly lower ΔV as well as a much longer TOF. The trajectory in Figure 13 is used as an initial guess to compute a transfer to a second EM L_2 southern halo orbit and the process is repeated for the remaining orbits of interest. The cost of associated with each of the three-burn EM-L_2 transfer trajectories are presented in Table 2. It

Table 2. EM-L_2 transfer ΔV costs

Orbit No.	ΔV_2 (m/s)	ΔV_2 (m/s)	$\Delta V_2 + \Delta V_3$ (m/s)	TOF (days)
1	190.50	11.95	202.45	14.70
2	192.64	28.04	220.68	14.14
3	187.71	51.74	239.45	13.83
4	183.78	69.94	253.72	13.90
5	179.93	87.35	267.28	13.97
6	177.27	120.28	297.55	14.23
7	175.20	138.42	313.62	14.36
8	173.18	130.58	303.76	14.76

is significant to note that, unlike the Earth-L_1 transfers, the intermediate ΔV costs increases as the algorithm to compute Earth-L_2 steps through the EM L_2 southern halo family. The approximately two-week time of flight fluctuates by less than one day for this class of Earth-L_2 transfers, however.

Despite the relatively long times of flight associated with these Earth-L_2 trajectories, it is still possible to compute round trip Earth-L_2-Earth transfers that do not violate the 21-day maximum human trip duration constraint. As an example, a 14.3-day Earth-L_2 transfer is connected to an Earth-bound return leg using a circumlunar free return trajectory segment as an initial guess. A 21-day time of flight constraint is imposed to produce the resulting round trip transfer trajectory depicted in Figure 14. The total ΔV cost – not including ΔV_1 – is $\Delta V_2 + \Delta V_3 + \Delta V_4 = 1468$ m/s

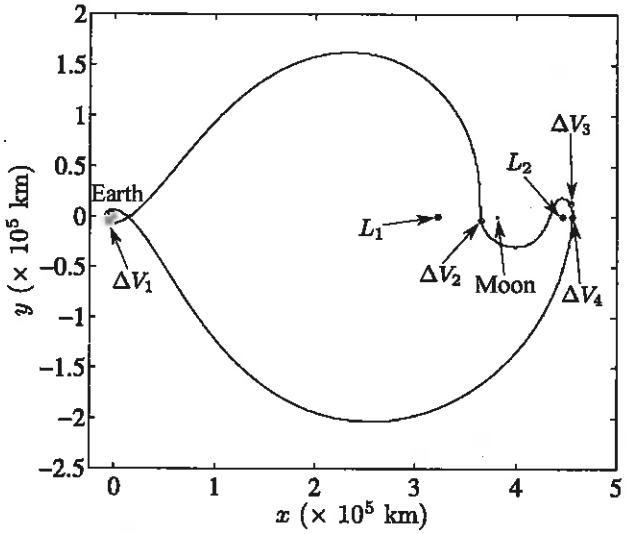

Figure 14. Example Earth-L_2-Earth transfer

with a large portion of the cost attributed to a 965 m/s burn required to depart the EM L_2 southern halo orbit to return to Earth.

TRANSFER RESULTS IN AN EPHEMERIS MODEL

While the transfers in the previous section are computed in the CR3B problem, these solutions may be transitioned into a higher-fidelity ephemeris model via differential corrections procedures. The CR3B model solutions are sampled at a selected time interval, and the resulting discretized solution is integrated within the ephemeris model. A multiple-shooting algorithm is employed to enforce full-state continuity along the transfer arcs and along the libration point orbit, although a velocity discontinuity between the transfer arc and the orbit is permitted. The transition to the ephemeris model can influences the characteristics of both the transfer and the libration point orbit. The effect of varying the inclination at LEO is also explored.

As a preliminary demonstration of the impact of lunar eccentricity, solar gravity, and Earth departure inclination on Earth-L_1/L_2 transfer trajectories, a direct, two-burn Earth-L_2 transfer is transitioned from the CR3B model and reconverged in a higher-fidelity ephemeris model as depicted in Figure 15. In this example, the ΔV cost for the ephemeris trajectories is fixed to be equal to the associated CR3B trajectory – 950 m/s. Recall that, in the CR3B model, the outbound legs of the transfer trajectories presented in this investigation are generally nearly planar. The trajectory in

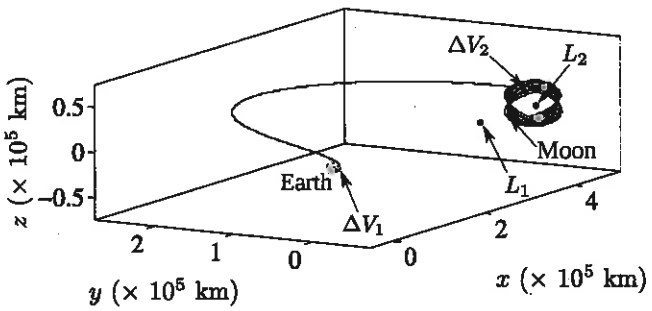

Figure 15. Example two burn Earth-L_2 ephemeris transfer

Figure 15 is computed with an epoch in mid-December 2017 when the lunar orbital plane is inclined approximately 20 degrees with respect to Earth's equatorial plane. Thus, to transition the CR3B trajectories to higher-fidelity transfers with an Earth departure inclination of 28.5 degrees (consistent with a launch from Kennedy Space Center), the trajectories in this analysis are first reconverged with a departure inclination of 20 degrees and a continuation procedure is implemented to increase the inclination to the desired angle.

An identical procedure is used compute three-burn Earth-L_1 transfers in a higher-fidelity Earth-Moon-Sun ephemeris model as well. A continuation procedure is again incorporated to raise the Earth departure inclination from 20 degrees to 28.5 degrees. To demonstrate the effects of Earth departure inclination on this particular collection of three-burn transfer trajectories, the ΔV costs for each trajectory in the continuation process are summarized in Table 3. To isolate, the effect of inclination, the time of flight and perilune altitude are fixed at 5 days and 400 km for each trajectory. The cost, ΔV_1 associated with departing Earth from a 200-km altitude parking orbit is also included

Table 3. Three-burn EM-L_1 ephemeris transfer ΔV costs

Inclination (deg)	ΔV_1 (m/s)	ΔV_2 (m/s)	ΔV_3 (m/s)	$\Delta V_2 + \Delta V_3$ (m/s)
20	3151.40	235.63	364.37	600.00
22	3151.80	235.03	367.97	603.00
24	3151.13	239.02	367.48	606.50
26	3151.39	247.34	364.66	612.00
28.5	3151.96	259.26	358.74	618.00

in the table to illustrate that, in this instance, changing the inclination does not significantly alter the Earth departure maneuver. The final converged three-burn Earth-L_1 ephemeris transfer at an inclination of 28.5 degrees appears in Figure 16. The intermediate ΔV cost of $\Delta V_1 + \Delta V_2 = 618$ m/s represents only a 3% increase in cost compared to the initial transfer with an Earth departure inclination of 20 degrees and illustrates the inclination does not appear to have a significant effect on libration point orbit transfer cost for the cases examined in this investigation.

STATIONKEEPING RESULTS

Given the unstable nature of many EM L_1 and L_2 libration point orbits relevant to human space exploration, the stationkeeping method associated with maintaining these orbits can be as critical to the mission design process as the construction of the transfer trajectories themselves. Using the

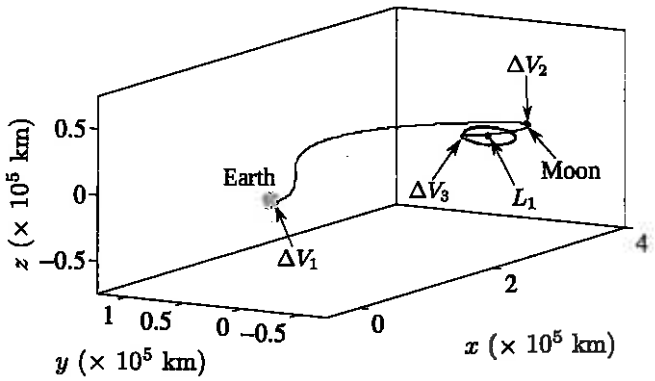

Figure 16. Example two burn Earth-L_1 ephemeris transfer

long-term stationkeeping strategy outlined previously, this investigation incorporates 16-revolution reference libration point orbits to maintain the desired orbit for 12 revolutions. The four unused revolutions effectively act as an "anchor" to ensure that the spacecraft maintains the same general behavior as the original reference solution. In this analysis, stationkeeping maneuvers are executed twice per orbit – approximately once per week, in general – at crossings of the x-z plane. Randomly-distributed navigation/modeling 1-σ errors of 1 km and 1 cm/s as well as 1% 1-σ maneuver execution errors are included to simulate the uncertainty associated with real-world stationkeeping operations. Monte Carlo simulation is implemented to make a preliminary assessment of the impact of libration point orbit type, size, and periodicity on stationkeeping cost.

Stationkeeping Costs Across Families of Periodic L_1/L_2 Orbits

Stationkeeping costs are first explored for several periodic EM L_1 and L_2 libration point orbits of potential relevance to human exploration activities. Each trajectory is maintained for 12 revolutions which is approximately 3.5 to 7.5 months for the trajectories considered here, but stationkeeping costs can reasonably be extrapolated for longer durations. Stationkeeping costs are estimated using 500-trial Monte Carlo simulations for each orbit of interest and the 12-revolution average ΔV_{tot} is extrapolated to produce an approximate annual stationkeeping cost. The costs associated with maintaining various EM L_1 and L_2 southern halo orbits are presented first in Figure 17. The highest average total stationkeeping cost of over 35 m/s is associated with the smallest EM L_1 southern halo orbit examined in Figure 17(a) with an orbital period of approximately 12 days. Conversely, maintaining the largest halo orbit tested required the lowest ΔV of approximately 3 m/s. Like the EM L_2 southern halo family, the larger the amplitude of the EM L_2 southern halo orbits, the lower the average total ΔV. However, it is important to observe in Figure 17(b) that the L_2 orbits are generally less costly to maintain than their L_1 counterparts with average total ΔV costs ranging from 2.6 to 18.5 m/s for the selected EM L_2 southern halo orbits.

Annual stationkeeping costs for selected members of the EM L_1 Lyapunov and vertical families appear in Figure 18. Similar trends are observed in both the Lyapunov and vertical orbits in that the largest amplitude trajectory requires the lowest average total ΔV. The smallest y-amplitude Lyapunov orbit requires the largest annual maintenance ΔV of any of trajectory in this investigation at over 39 m/s. Note that EM L_2 vertical orbits are not considered in this analysis because the trajectories' line of sight to the Earth is regularly blocked by the Moon which can be undesirable from a communications standpoint.

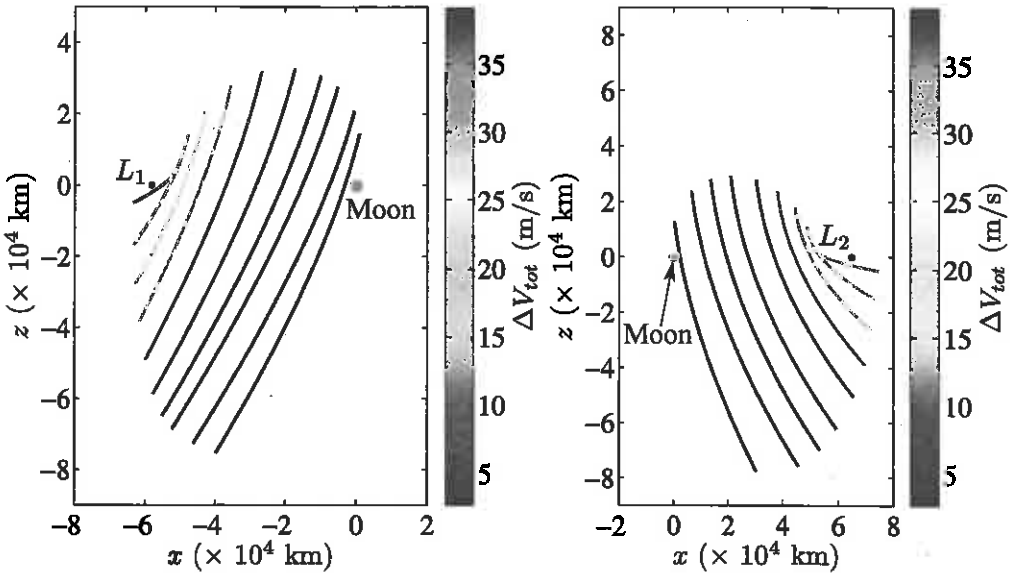

(a) EM L_1 southern halo family (b) EM L_2 southern halo family

Figure 17. SK costs for the EM L_1/L_2 southern halo families

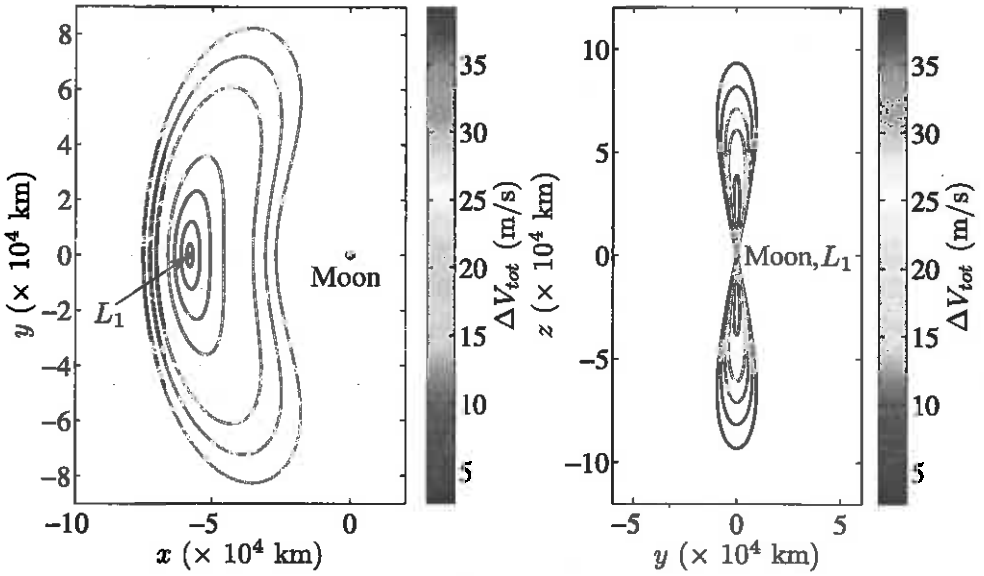

(a) EM L_1 southern halo family (b) EM L_2 southern halo family

Figure 18. SK costs for the EM L_1 Lyapunov and vertical families

Additional insight into the orbit maintenance costs depicted in Figures 17 and 18 is gained by exploring the correlation between the orbit stability index, ν, and annual stationkeeping ΔV costs.

The orbit stability index is computed as

$$\nu = \frac{1}{2}\left(|\lambda_{max}| + \frac{1}{|\lambda_{max}|}\right) \tag{3}$$

where λ_{max} represents the largest eigenvalue of the monodromy matrix associated with a particular periodic orbit.[11] Fundamentally, a larger stability index indicates greater instability in a periodic orbit while a stable periodic orbit corresponds to $\nu = 1$. The stability index is plotted against the annual stationkeeping costs for each of the four periodic families explored previously in Figure 19. First, note that for each family, the stability index decreases as the family goes larger which means

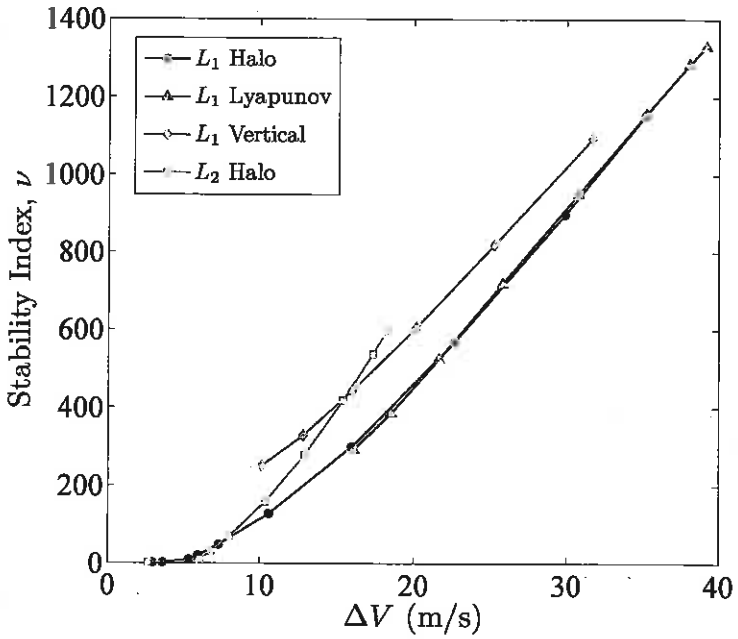

Figure 19. Effect of stability index, ν, on stationkeeping costs

that the orbits become less unstable. Orbit maintenance cost and stability index are clearly correlated and it is apparent that, as periodic orbits within the family become less unstable, their required stationkeeping ΔV goes decreases. Lastly, combining the stationkeeping results with the transfer results earlier, it can be said that, for the EM L_1 southern halo orbits, both transfer and stationkeeping costs decrease as the family grows. Conversely, stepping through the EM L_2 southern halo family results in higher transfer costs, but lower stationkeeping ΔV requirements.

Quasi-periodic Orbit Stationkeeping Costs

In addition to the analyzing the costs required to maintain various periodic orbits in the EM system, it is also beneficial to explore stationkeeping costs for associated quasi-periodic behavior because (1), mission requirements may only require a spacecraft to remain in the general vicinity of a libration point, as opposed to having to rigidly adhere to a periodic orbit and (2), in full-fidelity models, libration point orbits will inherently be quasi-periodic due to perturbations such as lunar eccentricity and solar gravity. Figures 20(a) and 20(b) illustrate the stationkeeping costs associated with maintaining EM L_1 and L_2 southern quasi-halo trajectories, respectively. For the each of the

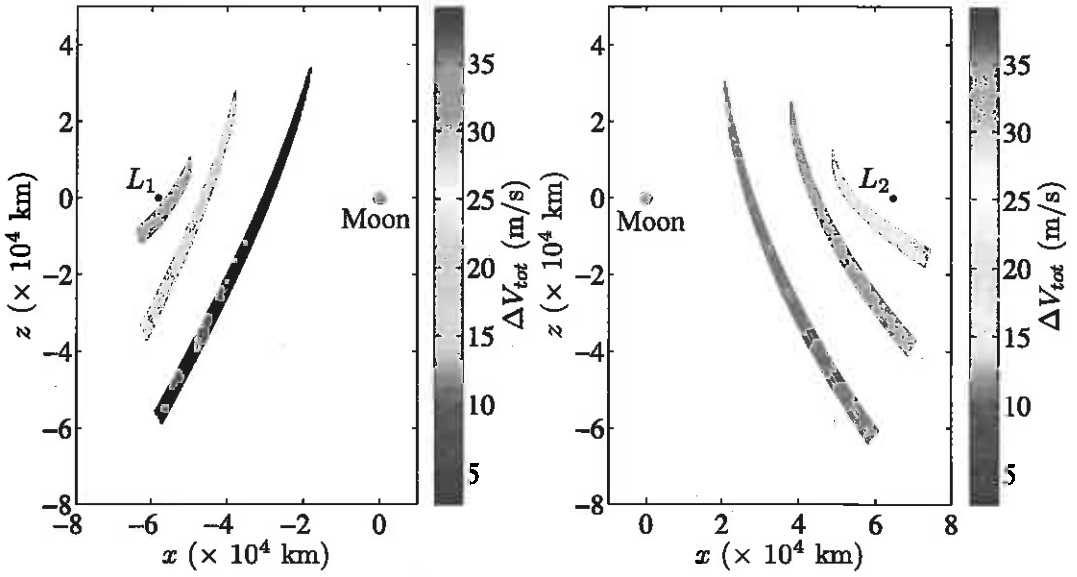

(a) EM L_1 southern quasi-halo family

(b) EM L_2 southern quasi-halo family

Figure 20. SK costs for the EM L_1/L_2 southern quasi-halo families

quasi-periodic trajectories simulated, the observed stationkeeping costs are very similar to the costs required to maintain the associated periodic orbits. This is not a completely unexpected result, but, nevertheless, it is important to confirm that periodic orbit maintenance costs can provide reasonable predictions for the ΔV required to maintain nearby quasi-periodic trajectories.

CONCLUSIONS

This research represents a preliminary investigation into transfer trajectory design options between the Earth and Earth-Moon L_1 and L_2 libration point orbits that may be relevant to future human space exploration activities. Both direct transfers and those incorporating close lunar passage are examined. Direct transfers provide relatively fast transport to orbits in the vicinity of L_1 and L_2, however, total ΔV costs vary greatly with orbit type. Generally, cost to transfer may be decreased by inserting onto nearly a planar revolution along 'large' quasi-periodic (quasi-halo and Lissajous) orbits. Increasing the energy level (decreasing C) additionally decreases the required ΔV to transfer. To further decrease ΔV costs for cases where time-of-flight is less important, it is useful to incorporate stable manifolds as a segment of the transfer.

Three-burn, lunar assisted transfers are developed to both EM L_1 and L_2 that leverage existing lunar free return trajectories solutions as part of an initial guess architecture. For the classes of three-burn transfer trajectories considered in this investigation, EM L_1 is reached more quickly than EM L_2, but at a higher ΔV cost. Examples of round trip Earth-L_1/L_2-Earth trajectories are presented to demonstrate that either EM L_1 or L_2 can be accessed within the 21-day total time of flight limit. Both Earth-L_1 and Earth-L_2 transfers are reconverged in a higher-fidelity model to demonstrate that these orbit architectures are valid in real-world mission applications and that Earth departure inclination appears to have minimal effect on transfer ΔV costs.

Optimal periodic and quasi-periodic orbit stationkeeping costs are assessed using a previously

established long-term stationkeeping strategy and it is observed, for the families investigated, that lower amplitude trajectory generally require more ΔV to maintain. A summary of transfer and stationkeeping ΔV costs for EM L_1 and L_2 southern halo orbits are presented in Table 4. The transfer ΔV values do not include the initial Earth departure maneuver, ΔV_1. It is clear from the

Table 4. Summrary of EM L_1/L_2 transfer and SK ΔV costs

	EM L_1 Direct	EM L_2 Direct	EM L_1 Lunar-Assisted	EM L_2 Lunar-Assisted
z-amp (km)	5000	5000	5000	5000
TOF (days)	3.99	6.41	4.87	14.70
ΔV (m/s)	609.07	957.24	515.83	202.45
Perilune alt. (km)	N/A	N/A	200	200
SK ΔV (m/s/yr)	35.18	18.25	35.18	18.25

analysis presented herein that the choice between the two venues, Earth-Moon L_1 and L_2, can be made on the basis of scientific and/or exploration goals without being limited, in most cases, by dynamical constraints of the Earth-Moon system.

ACKNOWLEDGMENTS

The authors recognize and appreciate the support for efforts at Purdue under NASA contract NNX12AC57G and the NASA Space Technology Research Fellowship (NSTRF) under NASA Grant No. NNX11AM85H.

REFERENCES

[1] M. Woodard, D. Folta, and D. Woodfork, "ARTEMIS: The First Mission to the Lunar Libration Points," *21st International Symposium on Space Flight Dynamics*, Toulouse, France, October 2009.

[2] D. Folta, M. Woodard, and D. Cosgrove, "Stationkeeping of the First Earth-Moon Libration Orbiters: The ARTEMIS Mission," *AAS/AIAA Astrodynamics Specialist Conference*, Girdwood, Alaska, August 2011. Paper No. AAS 11-515.

[3] *The Global Exploration Roadmap*, NASA Report, 2011 [Accessed September 27, 2012]. `http://www.nasa.gov/pdf/591066main_GER_2011_for_release.pdf`.

[4] J. Olson et al., *Voyages: Charting the Course for Sustainable Human Space Exploration*, NASA Report, 2012 [Accessed September 24, 2012]. `http://www.nasa.gov/pdf/657307main_Exploration%20Report_508_6-4-12.pdf`.

[5] M. Raftery and A. Derechin, "Exploration Platform in the Earth-Moon Libration System Based on ISS," *63rd International Astronautical Congress*, Naples, Italy, October 2012. Paper No. IAC-12-B3.1.

[6] V. Szebehely, *Theory of Orbits: The Restricted Problem of Three Bodies*. Academic Press Inc., New York, 1967.

[7] R. Farquhar and A. Kamel, "Quasi-Periodic Orbits about the Translunar Libration Point," *Celestial Mechanics*, Vol. 7, 1973, pp. 458–473.

[8] D. Richardson and N. Carey, "A Uniformly Valid Solution for Motion about the Interior Libration Point of the Perturbed Elliptic-Restricted Problem," *Astrodynamics Specialist Conference*, Nassau, Bahamas, July 1975. Paper No. AAS 75-021.

[9] K. Howell and H. Pernicka, "Numerical Determination of Lissajous Trajectories in the Restricted Three-Body Problem," *Celestial Mechanics*, Vol. 41, No. 1-4, 1988, pp. 107–124.

[10] E. Kolemen, J. Kasdin, and P. Gurfil, "Dynamics and Mission Design Near Libration Points, Vol. III: Advanced Methods for Collinear Points," *New Trends in Astrodynamics and Applications III, AIP Conference Proceedings*, Vol. 886, 2007, pp. 68–77.

[11] D. Grebow, "Generating Periodic Orbits in the Circular Restricted Three-Body Problem with Applications to Lunar South Pole Coverage," M.S. Thesis, School of Aeronautics and Astronautics, Purdue University, West Lafayette, Indiana, 2006.

[12] G. Gómez, À. Jorba, J. Masdemont, C., and Simó, *Dynamics and Mission Design Near Libration Points, Vol. III: Advanced Methods for Collinear Points*. World Scientific Co., River Edge, New Jersey, 2001.

[13] T. Pavlak and K. Howell, "Strategy for Optimal, Long-Term Stationkeeping of Libration Point Orbits in the Earth-Moon System," *AIAA/AAS Astrodynamics Specialist Conference*, Minneapolis, Minnesota, August 2012. Paper No. AIAA-2012-4665.

[14] E. Perozzi and A. Di Salvo, "Novel spaceways for reaching the Moon: an assessment for exploration," *Celestial Mechanics*, Vol. 102, 2008, pp. 207–218.

[15] R. Rausch, "Earth to Halo Orbit Transfer Trajectories," M.S. Thesis, School of Aeronautics and Astronautics, Purdue University, West Lafayette, Indiana, 2005.

[16] J. Parker and G. Born, "Direct Lunar Halo Rrbit Transfers," *AAS/AIAA Spaceflight Mechanics Conference*, Sedona, Arizona, January 2007. Paper No. AAS 07-229.